Influence of Constitutive Equations and Calculation Methods on the Results of Inelastic Analysis of Benchmark Problems

A.W.A. Konter

*TNO, Institute for Mechanical Constructions,
P.O. Box 29, NL-2600 AA Delft, The Netherlands*

G.M.A. Kusters

*TNO, Institute for Building Materials and Building Structures,
P.O. Box 49, NL-2600 AA Delft, The Netherlands*

SUMMARY

The major difficulty in obtaining realistic structural analysis results in high-temperature technology stems from the accurate characterization of the material behaviour given by the constitutive equations. In this paper several constitutive equations will be used to analyse the structural behaviour of a simply supported beam and circular plate loaded at its center, both tested at 1100 ^{o}F. The time-independent plastic behaviour has been analysed with the isotropic and kinematic hardening model as well as with the ORNL 10th cycle model and the fraction model of Besseling. The time-dependent creep behaviour has been analysed using the isotropic hardening rules and the ORNL auxilary hardening rules. No interaction of the creep and plastic behaviour was taken into account.

Especially for cyclic loading conditions, large differences occur in the predictions of the inelastic behaviour. Good agreement between theory and prediction can be obtained with models which accurately account for the ratio of kinematic and saturating isotropic hardening of the used material.

1. Introduction

Structural behaviour in high temperature technology is predicted mostly using the finite element method. The computer programming of this (non-linear) analysis method is complex and has to be verified with extreme care. In performing a realistic inelastic analysis it is, however, not sufficient to apply a verified computer programme. The results obtained depend strongly upon the constitutive equations used in modeling non-linear material behaviour such as plasticity and creep.

At TNO an extensive verification of constitutive equations has been carried out on two materials (nearly similar to AISI 304 and 2¼ Cr 1 Mo steel) frequently applied in nuclear technology. It was established that good results could be obtained with description based on the socalled fraction model of Besseling |1| both for plastic |2| and creep behaviour |3|. The resulting consitutive equations have been implemented in the general purpose programme DIANA (developed at TNO).

Having obtained verified constitutive equations and a verified computer programme, the next step is to demonstrate that the structural response of components can be analysed accurately. Corum et al. |5| have presented a number of benchmark test problems. In this paper the influence of the used constitutive equation will be presented. The analysis results will be restricted to the prediction of the structural behaviour of the simply supported beam and the circular plate tests. Both tests have been performed at 593 ^{O}C (1100 ^{O}F) and have been initiated to demonstrate the cyclic plastic and creep behaviour of components.

2. Analysis Technique

The analysis results have been obtained using the TNO general purpose programme DIANA. The mathematical descriptions for creep and plasticity implemented in this programme are based on the fraction model of Besseling |1|. Beside the good agreement between experiment and prediction, the model has the advantage that it is a general model and that other frequently applied models can be obtained in choosing a suitable set of model parameters. Although the model can describe non-isothermal effects, we will restrict ourselves in this paper to constant temperature analysis. Furthermore, the possibility of the model to describe viscoplasticity will not be dealt with in this paper.

The basic idea of Besseling is the subdivision of an infinitisimal volume element into a number of (volume) fractions with different material properties. Each of these fractions may exhibit elastic, plastic and/or creep behaviour. The behaviour of a fraction is completely isotropic and can consequently be described by the classical isotropic formulation for creep and plasticity. All fractions are assumed to have the same total deformation, while the elastic, plastic and creep strains are different. Thus, a set of internal stresses is introduced which can describe non-isotropic effects like the Bauschinger effect.

Using the classical isotropic description for each volume fraction k the rate equation for the stress vector $\dot{\sigma}^k$ is given by

$$\dot{\sigma}^k = S \mid \dot{\varepsilon} - \dot{\varepsilon}_p^k - \dot{\varepsilon}_c^k \mid \qquad (1)$$

in which S is a matrix of elasticity constants, $\dot{\varepsilon}$ the total strainrate vector, $\dot{\varepsilon}_p^k$ the plastic strainrate vector and $\dot{\varepsilon}_c^k$ the creep strainrate vector. Requiring that, in case of plasticity, the stress of a fraction has to satisfy the yield criterion of fraction k leads to the introduction of yield matrices Y^k.

$$\dot{\sigma}^k = | S - Y^k | | \dot{\varepsilon} - \dot{\varepsilon}_c^k | \quad (2)$$

As a direct consequence of the assumption that the total deformation of every fraction, each with its own material properties, has to be equal in magnitude, the stresses of each fraction are different. The stressrate vector of an infinitisimal volume element can be obtained by summing the stressrate vectors of the separate fractions each with their relative volume ψ^k (with $\sum_{k=1}^{n} \psi^k = 1$).

$$\dot{\sigma} = \sum_{k=1}^{n} \psi^k \dot{\sigma}^k = | S - \sum_{k=1}^{n} \psi^k Y^k | | \dot{\varepsilon} - \dot{\varepsilon}_c^k | \quad (3)$$

Equation (3) can be implemented in the usual way in a finite element programme |4|. The procedure is quite analogue to the one based on isotropic behaviour which can be found in |6| for instance. In literature the fraction model is sometimes referred to as overlay model |6|. By using an overlay technique the component is analysed by a number of layers, giving each layer different material properties. It is obvious that this can be done only in the case of plane 2-dimensional components. The fraction model, however, is basically a 3-dimensional theory which can be applied to 3-dimensional problems. Moreover, even in 2-dimensional problems the fraction model is different from the overlay model, due to the interaction of stress and strain components in the direction normal to the plane which is considered.

In solving the non-linear problem given by equation (3) an incremental solution method is required. Within an incremental load/time step several methods are available for calculating the incremental displacements (constant and tangential stiffness matrix methods) as well as iteration techniques within the load/time step to improve the obtained displacement increment (constant stiffness, Newton-Raphson and modified Newton-Raphson). Note, however, that equation (3) is a differential equation which is being solved numerically and hence the obtained solution depends upon the size of the (load/time) step, even when use is made of the most advanced solution technique.

In the results presented in this paper, we have chosen the tangential stiffness matrix method and Newton-Raphson iteration technique, which means that the stiffness matrix is assembled and inverted during each step and iteration. Convergence has been controlled by an energy criterion. The maximum number of iterations within a load/time step was taken to be five.

3. Constitutive Equations

Inelastic phenomena at elevated temperature are mostly described by treating the plastic and creep strain separately (Maxwell type description). This means that time-independent inelastic deformation will be referred to as plastic deformations while the time-dependent deformations are denominated as creep deformations. In this description the stress acting on the mechanism responsible for creep deformations, is equal to the stress acting on the plastic mechanism. Interaction of creep and plasticity is introduced by modifying the plasticity hardening rules with a function of the creep strain and/or the creep hardening rules by a plastic strain dependency.

Another basically different method is assuming that the plastic strain is equal to be creep strain, resulting in different stresses acting on creep and plastic mechanisms (Bingham type description or viscoplasticity). Interaction of creep and plasticity always occurs in this case.

In the present paper only elevated temperature tests will be analysed. It appears that for the used material (AISI 304) the inelastic behaviour at this temperature can best be approximated by a Maxwell type behaviour. No interaction is introduced in the present analysis results, although some material test indicate that interaction occurs for the higher stress levels |7|.

The plastic behaviour has been investigated using the isotropic and kinematic hardening rule as well as the ORNL 10th cycle model and the fraction model. All parameters have been based on the bilinear approximations of the cyclic stress strain curve, shown in figure 1a. The isotropic model is obtained using one elastic plastic fraction (figure 1b); the kinematic model (fig. 1c) can be obtained using one elastic and one elastic-ideal plastic fraction (the plastic tangent modulus is then determined by the relative volume of the fractions). The ORNL 10th cycle model (fig. 1d) is identical to the kinematic model except that before a load reversal the yield stress is updated. For the fraction model (fig. 1e) also a bilinear approximation has been chosen and hence 2 fractions are sufficient. The model is a combination of kinematic and (saturating) isotropic hardening. The use of more fractions gives a better description of the curvature in the tensile curve and can take into account the fact that cyclic hardening depends upon the applied strain range.

In the present paper the description of creep effects is restricted to two different models. Firstly the creep behaviour is assumed to be completely isotropic (denominated with isotropic creep hardening). Secondly the ORNL auxilary rule |7| has been applied, which gives better results in case of load reversals. Although the fraction model gives a quantitatively better description of creep effects under arbitrary load conditions |3|, the effect of this formulation in structural behaviour is not investigated in this paper.

The function describing the scalar creep strain ε^c which has been used in the analyses depends upon a scalar stress σ and the time t.

$$\varepsilon^c = \varepsilon_T \ (1 - e^{-Rt}) + \varepsilon_t \ (1 - e^{-rt}) + \dot{\varepsilon}_s t \qquad (4)$$

in which

$\varepsilon_T = \varepsilon_t = 6{,}7 \ 10^{-6} . \sigma$ |mm/mm|

$R = 1{,}2 \ 10^{-2}$ $|h^{-1}|$

$r = 1{,}1 \ 10^{-3}$ $|h^{-1}|$

$\dot{\varepsilon}_s = A \ \sigma^n = 4{,}4 \ 10^{-21} \sigma^{7,3}$ $|mm/mm.h^{-1}|$

This function has been chosen to give a reasonable fit in the investigated range of (interpolated) experimental results |5|. Changing of the creep strain rate due to a change in stress level is accounted for by a strain hardening hypothesis which appear to give the best results for this material (AISI 304). The description of the creep strain is rather poor, especially the primary creep strain part in (4). Good interpretation of the results is difficult, because in the low stress region hardly any creep strain occurs within a reasonable time, while for higher stresses the subdivision of plastic and creep strain is not always clear. For analysing the structural behaviour of a component especially the creep behaviour at low stresses is important.

Multiaxial creep and plastic behaviour is accounted for by a Von Mises yield criterion and flow rule.

4. Analysis Results

The geometry and mesh division of the beam are shown in figure 2. The element mesh contains 58 quadrilateral 8 node plane stress elements. The load histories of two load controlled beam tests (coded analogue to |5|: Beam B9 and Beam B10) are depicted in figure 3. The test consisted of elastic-plastic short time cycling, denoted with time-independent behaviour,and of time-dependent creep behaviour. In presenting the results the displacements (predicted or experimental) have been subdivided accordingly.

Beam B9 has been analysed using 6 descriptions of material behaviour. Both the isotropic and ORNL creep hardening rule have been combined with the isotropic, kinematic and fraction model for plasticity. The results of the time-independent response during creep cycling are plotted in figure 4, the time-dependent response in figure 5. Note that different plasticity models had no influence on subsequent creep behaviour. The time-independent response of the post creep cycle is shown in figure 6. The elastic plastic behaviour during the post creep cycle has not been affected by the different creep hardening rules in the previous period.

Beam B10 has been analysed using the isotropic creep hardening rule combined with the isotropic, kinematic, ORNL 10th cycle model and fraction model for plasticity. Figure 7 shows the experimental and predicted load displacement diagrams for the 10 pre-creep cycles. Figure 8 compares the results of the time-independent behaviour during the creepcycle. The predicted time-dependent response is identical to the response obtained with the analysis of Beam B9 (figure 4).

The geometry and mesh division of circular plate are shown in figure 9. The element mesh contains 72 quadrilateral 8-node axi-symmetric elements. The deflection controlled experiment CP4 with deflection history shown in figure 10, has been analysed. The isotropic creep hardening rule has been used in combination with the isotropic and kinematic hardening rule for plasticity. Figure 11 shows the predicted and experimental load deflection response while figure 12 reflects the time-dependent response.

5. Discussion

If no load reversals are being applied, no differences occur in the predictions of structural behaviour for the used different models of material behaviour.

In the (load-controlled) beam analysis the use of different models of plasticity did not influence the subsequent creep behaviour. The deflection controlled plate analysis resulted in a different creep behaviour depending on the hardening model for plasticity.

The first creep period (traject 2-3 in figure 3) in the beam analysis resulted in a stress distribution with an initially elastic response during the subsequent load increase.

The application of different hardening rules influences the prediction of the beam experiments considerably in case of load cycling. With the kinematic model the same time-independent response is found during each cycle independent of the previous load history. The isotropic model results in a linear elastic behaviour after a number of cycles. The ORNL 10th cycle model and fraction model are combinations of both types of hardening. In the ORNL model the yield stress can be updated before each load reversal or as a function of the accumulated plastic strain, which will improve the results. The main difference between both models is that in the ORNL model the initial load curve is assumed to behave kinematic, while in the 2-fraction model the initial load curve is a combination of isotropic and kinematic hardening. Thus internal stresses caused by initial loading will be different for both models. Generally the agreement between experimental time-independent response and predictions based on the fraction model is good.

The main difference between experimental and the predicted results seem to be caused by inaccurate modeling the plastic behaviour and/or the creep behaviour and not by the interaction of creep and plasticity.

6. Acknowledgement

This work was commissioned by the Project Group of Nuclear Energy TNO. The authors thank the Project Group and the Dutch Ministry of Economic Affairs for the permission to publish this paper.

References

|1| Besseling, J.F. "A theory of elastic, plastic and creep deformation of an initially isotropic material showing strain hardening, creep recovery and secondary creep." J. Appl. Mech., Vol. 25, No. 4, Dec 1958, pp 529-536.

|2| Janssen, G.T.M., Huetink, J. "Experimental Verification of Constitutive Equations for Plasticity under Biaxial, Cyclic and Non-radial Loading Conditions". Proc. 6th Int. Conf. on Structural Mechanics in Reactor Technology, paper L 4/2, Paris, France (August 17-21, 1981).

|3| Roode, F., Dortland, W. "Experimental Verification of Constitutive Equations for Creep and the Interaction of Creep and Plasticity under Biaxial Loading Conditions." Proc. 6th Int. Conf. on Structural Mechanics in Reactor Technology, paper L 4/1, Paris, France (August 17-21, 1981).

|4| Kusters, G.M.A., Huetink, J. "Theoretical backgrounds for the performance of inelastic analyses based on the fraction model with DIANA-NONLIN." TNO-IBBC report nr. BI-79-34/68.2.1211 (in Dutch).

|5| Corum, J.M., Wright, W.B. "Pressure Vessels and Piping: Verification and Qualification of Inelastic Analysis Computer Programs", ASME, New York, 1975.

|6| Zienkiewicz, O.C. "The Finite Element Method", Mc. Graw-Hill, London, 1977.

|7| Corum, J.M. et al. "Interim Guidelines for Detailed Inelastic of High-Temperature Reactor System Components", ORNL-5014, December 1974, Oak Ridge National Laboratory, Oak Ridge, Tenn.

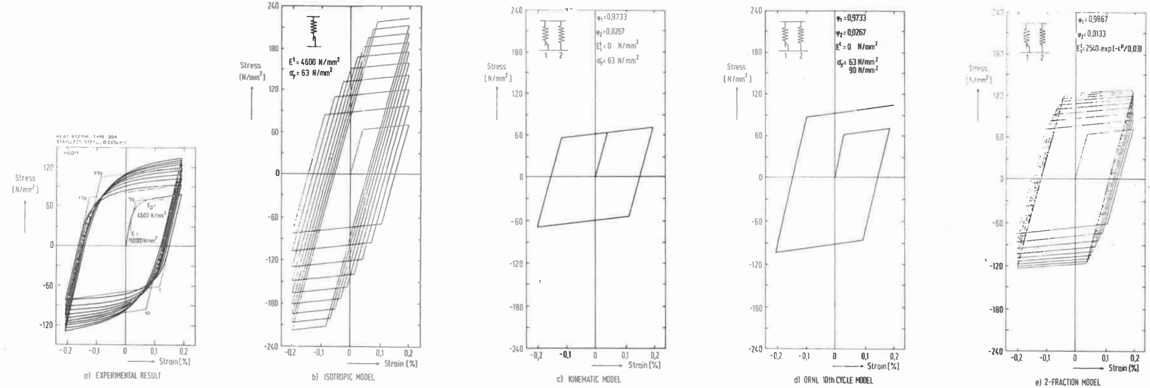

Figure 1   Comparison of plasticity hardening rules.

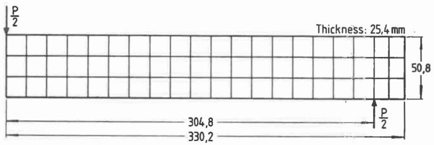

Figure 2   Finite element mesh beam.

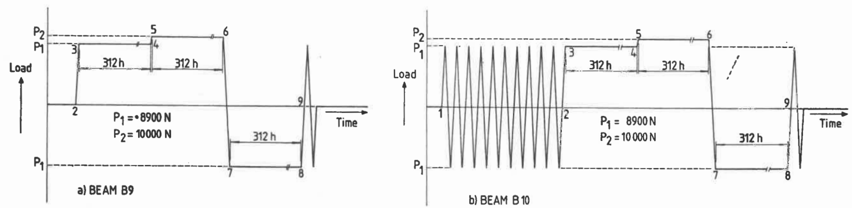

Figure 3   Histograms for load-controlled beam analysis.

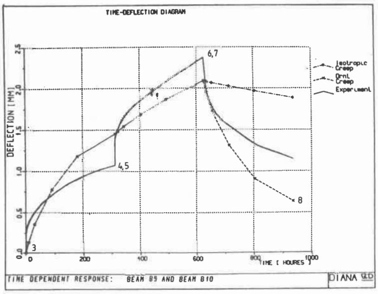

Figure 4 Comparison of measured and predicted time dependent response during cyclic creep period.

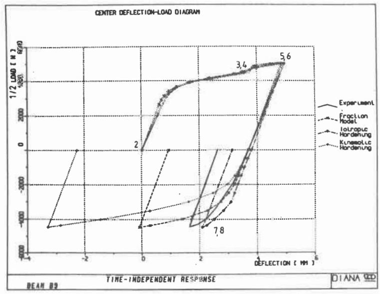

Figure 5 Comparison of measured and predicted time independent response during cyclic creep period.

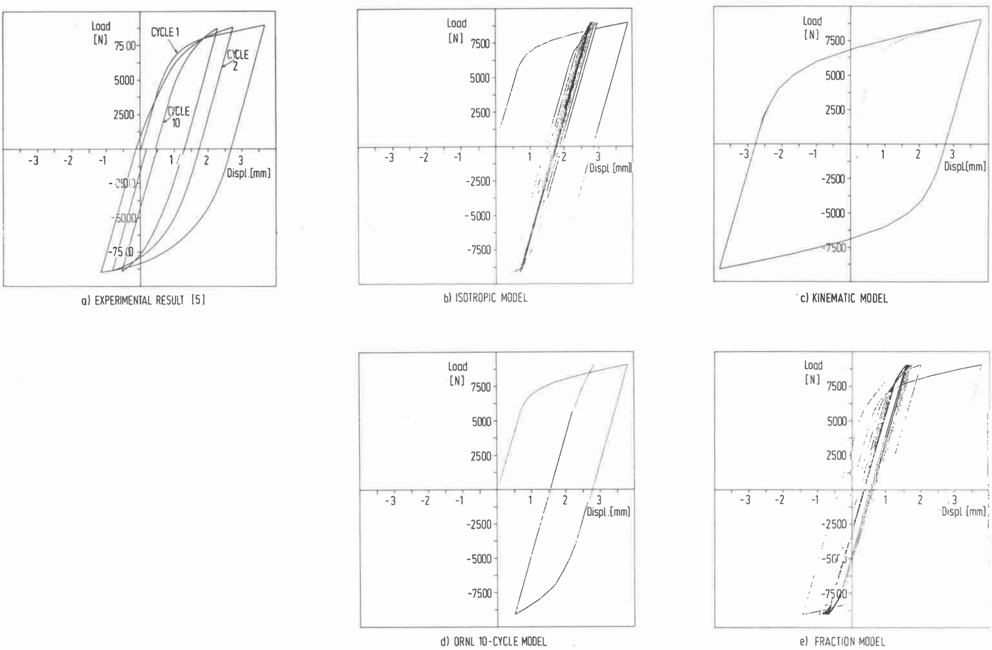

Figure 7 Comparison of measured and predicted response for Beam B10, pre-creep cycles.

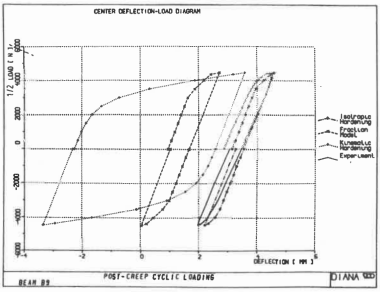

Figure 6 Comparison of measured and predicted response, post-creep cycle.

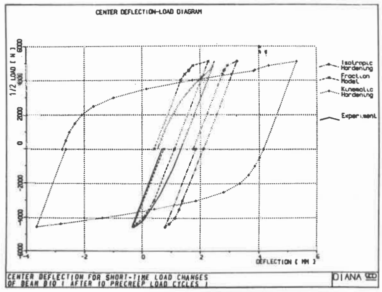

Figure 8 Comparison of measured and predicted time independent response during cyclic creep period.

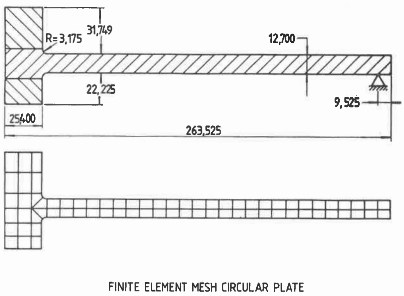

Figure 9 Finite element mesh circular plate.

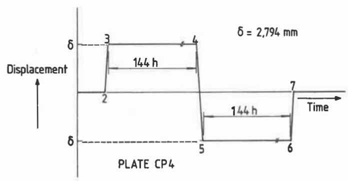

Figure 10 Histogram for deflection-controlled plate analysis.

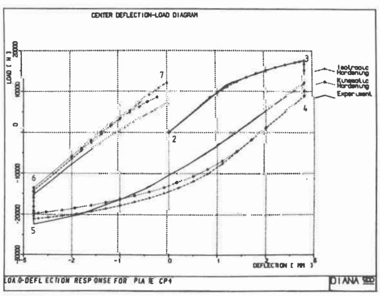

Figure 11 Comparison of measured and predicted load-deflection response.

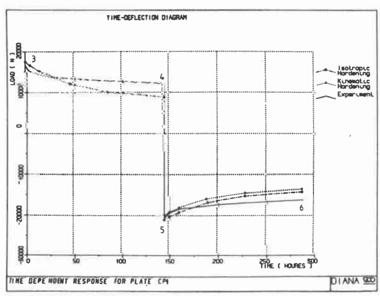

Figure 12 Comparison of measured and predicted load-time response.